

# An equivalent complex permeability model for litz-wire windings

Xi Nan  
C. R. Sullivan

Found in *Fortieth IEEE Industry Applications Society Annual Meeting*, Oct. 2005, pp. 2229–2235.

©2005 IEEE. Personal use of this material is permitted. However, permission to reprint or republish this material for advertising or promotional purposes or for creating new collective works for resale or redistribution to servers or lists, or to reuse any copyrighted component of this work in other works must be obtained from the IEEE.

# An Equivalent Complex Permeability Model for Litz-Wire Windings

Xi Nan and Charles R. Sullivan

xi.nan@dartmouth.edu

charles.r.sullivan@dartmouth.edu

http://engineering.dartmouth.edu/inductor

8000 Cummings Hall, Dartmouth College, Hanover, NH 03755, USA, Tel. +1-603-646-2851 Fax +1-603-646-3856

**Abstract**—Previous methods for calculating power loss in litz-wire windings usually assume very fine strands such that the diameter of strands is much smaller than skin depth. In this paper, we present a method for calculating proximity-effect loss in litz-wire windings. This method uses an equivalent complex permeability model of the winding to describe the proximity effect. We first obtain a permeability model for litz-wire bundles, then use homogenization techniques to find the average permeability of a winding. Permeability models are provided for bundles consisting either rectangularly packed or hexagonally-packed strands. The permeability model enables high-accuracy proximity-effect loss analysis and field analysis for litz-wire windings at high frequencies. It can also be used to find the leakage inductances in magnetic components.

## I. INTRODUCTION

Eddy-current effects, including skin effect and proximity effect, increase power loss in windings at high frequencies dramatically. Accurately analyzing eddy-current loss is very important in the design and optimization of power components. Litz wire is often used in power components to reduce the skin-effect loss and obtain lower total loss at higher frequencies. Previous AC winding loss calculation methods for litz-wire windings are mostly based on the assumption of very fine strands, such that the diameter of strands is much smaller than a skin depth [1], [2], [3]. References [4] and [5] apply the Bessel-function method to litz-wire windings to approximate eddy-current loss in a wider frequency range. However, the Bessel-function method uses the analytical field solution for an isolated round wire subjected to an external field to approximate the behavior of a round wire in a winding. It is only a good approximation when the wires are far apart from each other, which is not true for litz-wire strands and it produces large error for solid-wire windings [6]. Numerical analysis can be used to obtain loss results to any desired accuracy, but it is very time consuming, especially for a litz-wire winding, which may contain thousands of small strands. Based on high-accuracy finite element analysis (FEA) results, a model for the proximity-effect loss in round-wire windings was given in [6], [7]. However, it cannot be applied directly to litz-wire windings at high frequencies due to the special winding geometry of litz-wire windings. In this paper, we present a model for calculating proximity-effect loss in litz-wire windings for a wider frequency

range by deriving an equivalent permeability model for litz-wire windings from the proximity-effect loss model in [7].

The proximity-effect loss model is presented in terms of a proximity-effect loss factor, which is power loss per length normalized to the square of external field magnitude [7]. The proximity-effect loss factor describes the eddy current loss caused by an external time-varying field in a conductor matrix consisting of repeating cells of round conductors (with space between each). To model proximity effect in such a wire matrix, the conductor matrix can also be considered as a block of nonconductive material with complex permeability [8], [9]. The complex permeability of the winding can be derived from the proximity-effect loss model based on the relationship between power loss and the imaginary part of permeability using the physical relationship between real and imaginary permeability [10]. The complex permeability model, like the proximity-effect loss model in [7], separates the overall field analysis from the local eddy-current analysis in each conductor. Furthermore, the complex permeability model contains information about how the local eddy currents affect the overall field distribution and can be help for solving the overall field distribution, especially in a winding with two-dimensional (2-D) geometry such as a litz-wire winding.

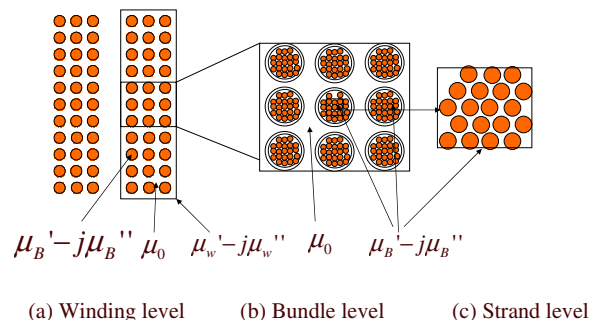


Fig. 1. The modelling process for a litz-wire winding

In a litz-wire winding, as shown in Fig. 1, conductors are arranged in a more complex pattern than in solid-wire windings; thus the equivalent complex permeability model for a litz-wire winding cannot be obtained directly from the proximity-effect

This work was supported in part by the United States Department of Energy under grant DE-FC36-01GO1106.

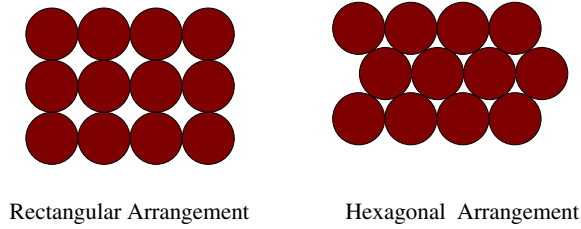


Fig. 2. Two ideal arrangements of conductors in a winding

loss factor for a solid-wire matrix. This is an eddy-current problem and can be solved using FEA.

Alternatively, the eddy-current field problem for high-frequency litz-wire windings can be solved by treating each bundle as a cylinder made of material with known permeability  $\mu'_B - j\mu''_B$ . Then, by magnetostatic field analysis and the aid of FEA, we can homogenize repeated cells of bundles and find the average permeability of a litz-wire winding  $\mu'_w - j\mu''_w$ . The complex permeability model for litz-wire windings can help us obtain a more accurate proximity-effect loss expression at high frequencies where the diameters of the strands are larger than the skin depth. Also, it helps us simplify an eddy current field computation problem to a problem similar to a magnetostatic problem but with all the quantities phasors and find the field distribution without solving for the local eddy current distribution inside each winding, which is much more time-efficient than direct FEA.

There are different possible packing patterns in windings [1] and also inside litz-wire bundles. To see how the different winding patterns affect proximity-effect loss, we investigate both the proximity-effect loss in rectangularly packed wires and hexagonally-packed wires (as shown in Fig. 2) and present loss models and permeability models for both. This investigation would also be useful for proximity-effect loss calculations in solid-wire windings.

In Section II, we review numerical simulation results of the complex permeability for solid-wire windings and how to derive complex permeability models from the proximity-effect loss factor model [10]; similar models for hexagonal windings are derived in Section III for the need of modelling different possible packing patterns in practical windings; In Section IV, we discuss the homogenization of the litz-wire bundles and the spaces between bundles as is needed for calculating complex permeability for litz-wire windings.

## II. COMPLEX PERMEABILITY MODEL FOR A SOLID-WIRE WINDING

In this section we review the complex permeability model for a solid-wire winding that was developed in [10]. The overall

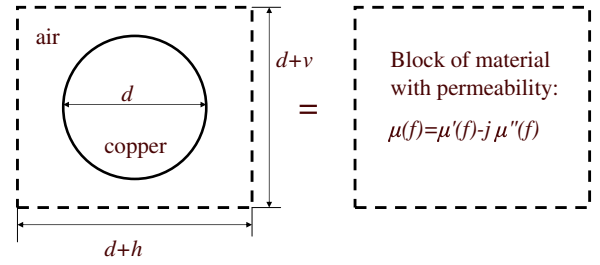


Fig. 3. Definition of complex permeability of a winding. The left half of the figure shows a cell of the cross section of a winding of round conductors with diameter  $d$ . The distance between each wire in the field direction is called  $v$  and the distance between wires in the other direction is defined as  $h$ ; the right half shows its equivalent at high frequencies—a block of material with permeability  $\mu' - j\mu''$ .

equivalent complex permeability of a winding is defined and calculated in [10] as:

$$\mu_e = \overline{B}/\overline{H} = \overline{B' + jB''}/(\overline{H' + jH''}) \quad (1)$$

where  $\overline{B}$  and  $\overline{H}$  are particular types of averages of  $B$  and  $H$ , chosen such that their ratio gives the effective permeability.  $\overline{B}$  is the total complex flux through the winding area divided by  $d + h$  and  $\overline{H}$  is the integration of complex  $H$  along the field direction divided by the length  $d + v$ .  $h$ ,  $v$  and  $d$  are defined in Fig. 3.

The overall complex permeability of a solid-wire winding can be obtained from numerical simulations in a setup as in Fig. 3. The FEA results for complex permeability shows that the real part of the relative permeability is one at low frequencies where the wire diameter is much smaller than skin depth [10]. At high frequencies, the real part of the complex permeability of the winding goes to a constant which depends on the winding geometry and the ratio between copper area and air area. The imaginary part of the complex permeability of the winding is approximately proportional to frequency  $f$  at low frequencies and proportional to  $f^{-0.5}$  at high frequencies. Different distances between wires in the same layer  $v$  change the distribution of eddy currents and change the equivalent permeability of one layer.

The imaginary part of the complex permeability  $\mu''$  is directly related to the power loss (or power dissipation) [9]. If a block of material with permeability  $\mu' - j\mu''$  is subjected to an external field with magnitude  $H_0$ :

$$P_v = \mu'' \omega H_0^2 \quad (2)$$

where  $P_v$  is power loss per unit volume.

Given a model of proximity-effect loss factor  $\hat{G}$ —defined as proximity-effect loss per unit length normalized by  $H_0^2$  and conductivity  $\sigma$  in [7]—and (2), the imaginary part of permeability is easily obtained:

$$\mu'' = \frac{\hat{G}}{2\pi f(d+h)(d+v)\sigma} \quad (3)$$

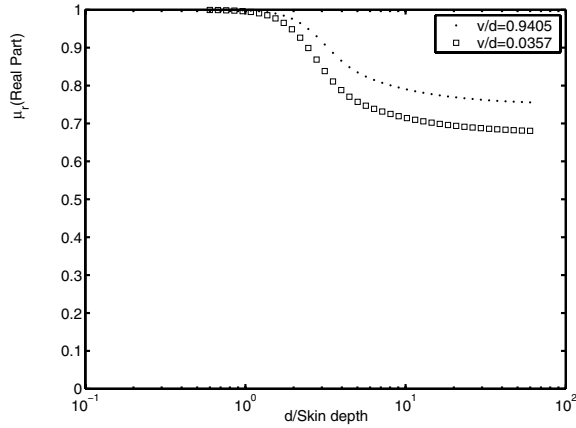


Fig. 4. Real part of relative permeability of two windings with different interwire distances  $v$  and the same interlayer distance  $h/d = 1.2619$

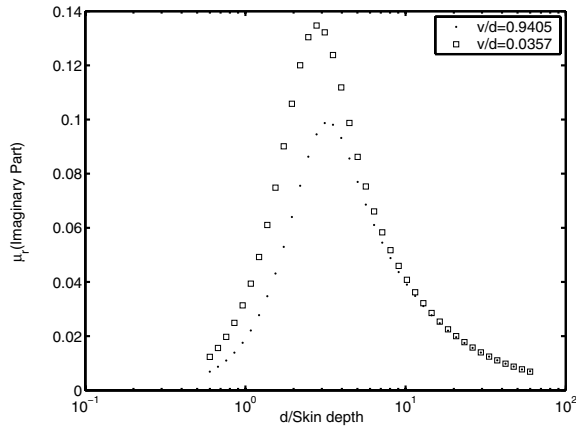


Fig. 5. Real part of relative permeability of two windings with different interwire distances  $v$  and the same interlayer distance  $h/d = 1.2619$

where  $\mu''$  is the imaginary part of the complex permeability of a winding in which the spacing between each wire parallel to the field direction is  $v$ , the spacing in the direction perpendicular to the field is  $h$  and the wire diameter is  $d$ .

Based on the proximity-effect loss factor model  $\hat{G}$  in [7] (also presented in the Appendix) and (3), the imaginary part of relative permeability is:

$$\mu_r'' = \frac{1}{2\pi\sigma f} \frac{1}{(d+h)(d+v)} \left[ (1-w) \frac{3\pi}{16} k^{-3} X \frac{\sinh(kX) - \sin(kX)}{\cosh(kX) + \cos(kX)} + w \frac{\pi}{32} \frac{X}{(X^{-3} + b^3)} \right] \quad (4)$$

$$X = \frac{d}{\delta} = d\sqrt{\pi\sigma\mu f} \quad (5)$$

where  $w$  is a weight function determined by winding geometry;  $k$  and  $b$  are also functions of winding geometry parameters  $v/d$  and  $h/d$ ,  $\sigma$  is the conductivity of wire material and  $\mu$  is permeability. Expressions for  $w$ ,  $b$  and  $k$  can be found in the

Appendix.

A physical relationship exists between real and imaginary permeability of material, which is called the Kramers-Kronig relation. The Kramers-Kronig relation, which states that real and imaginary parts of complex permeability are Hilbert pairs, is valid because of the causal connection between magnetization and magnetic field:

$$\mu'(\omega) = \frac{2}{\pi} \int_0^\infty \frac{\mu''(\eta)\eta}{\eta^2 - \omega^2} d\eta + \mu'_{const} \quad (6)$$

where  $\mu'_{const}$  is a constant determined by physical constraints.

The real part of complex permeability for a round wire is given as [10]:

$$\mu_r'(X) = 1 - \hat{\mu}_r'(0) + \hat{\mu}_r'(X) \quad (7)$$

where  $\hat{\mu}_r'(X)$  is a frequency-dependent component of the real part of relative permeability given by the Hilbert transform of (4):

$$\hat{\mu}_r'(X) = \frac{d^2}{16(d+h)(d+v)} \left[ w \frac{3b^5 X^5 (-1 + b^6 X^6) + 4\sqrt{3}(-1 + b^4 X^4)}{3b^2(-1 + b^{12} X^{12})} + (1-w) \frac{3\pi}{k^3 X} \frac{\sinh(kX) + \sin(kX)}{\cosh(kX) + \cos(kX)} \right] \quad (8)$$

### III. POWER LOSS MODEL AND COMPLEX PERMEABILITY MODEL FOR HEXAGONALLY PACKED WINDINGS

There are two types of ideal arrangements of round conductors in a winding: rectangular and hexagonal. It's difficult and unnecessary to accurately position the strands in a practical round litz-wire bundle in either of the ideal packing arrangements shown in Fig. 2, because usually there are a lot of very fine strands in litz-wire bundles. Practical litz wire very probably is a combination of these two packing patterns. So, it is useful to inspect the proximity-effect loss in both kinds of packing patterns.

We performed FEA simulations for eddy-current loss in a similar way as for solid-wire windings in rectangular packing [6]. To take insulation on wires and packing effects into account, we define  $d_0$  as the diameter of the area occupied by each wire, and  $d$  as the diameter of the actual copper area. We obtain proximity-effect loss results for a conductor as shown in Fig. 6. The proximity-effect loss factor for hexagonally packed windings is the same as that of a rectangularly packed winding at very low frequencies. At high frequencies, given two windings with the same wires and the same insulation but with a different packing pattern, the hexagonally packed winding has a larger proximity-effect loss factor. The difference in packing patterns has a larger effect on the proximity-effect loss when the distance between wires (the ratio between  $d_0$  and  $d$ ) is smaller. According to our FEA results, the difference in proximity-effect factor is around 10% for these two packing patterns at high frequencies where diameter is ten times of the skin depth and when  $d_0/d$  is 1.3.

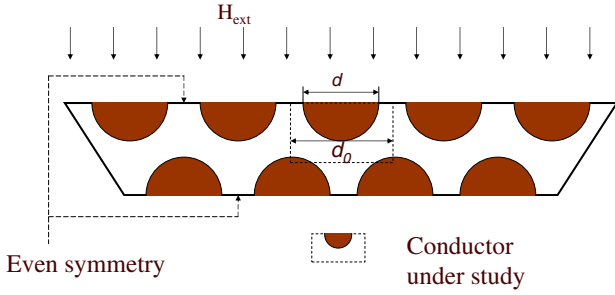


Fig. 6. FEA simulation configuration for a hexagonal winding

Proximity-effect loss factor  $\hat{G}_{hex}$  for a hexagonally packed winding is found by performing curve fit with a similar function form as that of the proximity-effect loss factor model for rectangularly packed windings to match the simulation data:

$$\hat{G}_{hex}(X) \cong (1 - w_{hex}) \frac{3\pi}{16} k_{hex}^{-3} X \frac{\sinh(k_{hex}X) - \sin(k_{hex}X)}{\cosh(k_{hex}X) + \cos(k_{hex}X)} + w_{hex} \frac{\pi}{32} \frac{X}{(X^{-3} + b_{hex}^3)} \quad (9)$$

The values of  $w_{hex}$ ,  $k_{hex}$  and  $b_{hex}$  are:

$$\begin{aligned} b_{hex}(\lambda) &= 0.1401e^{-1.4717\lambda} + 0.4284 \\ k_{hex}(\lambda) &= -0.2064\lambda + 1.5970 \\ w_{hex}(\lambda) &= 2.4555 \end{aligned} \quad (10)$$

where  $\lambda$  is defined as:

$$\lambda = d_0/d - 1 \quad (11)$$

The complex permeability model for hexagonally packed windings is similar to that for the rectangularly packed winding in (4) and (8). However, the area per wire  $d^2(1+v)(1+h)$  should be replaced by  $\sqrt{3}d^2(1+\lambda)^2/2$ , and  $b$ ,  $w$  and  $k$  should be replaced by  $b_{hex}$ ,  $w_{hex}$  and  $k_{hex}$ .

In practice, usually, an average packing factor  $F_p$  can be easily found from manufacturer's data or measurements for litz-wire bundles [2], which is defined as the ratio between copper area and area of a single bundle. However, the packing pattern is not specified. To use a complex permeability model for litz-wire bundles, the user must choose the packing pattern style (or combinations of packing patterns) and determine the geometric parameters  $d$ ,  $h$  and  $\lambda$  from the packing factor information. There are a few possible choices when determining these geometric parameters. We inspect how much difference in proximity-effect loss prediction might result from different choices of geometric parameters for the same numbers of strands and same packing factor.

For the same setups such as the same wire diameters and same insulation thicknesses, hexagonally packed windings have

a larger packing factor than rectangular windings have. In the ideal case, the packing factor  $F_{p,hex}$  of hexagonally packed winding is  $2/\sqrt{3}$  of that of a rectangularly packed winding  $F_{p,rec}$ :

$$F_{p,hex} = \frac{2}{\sqrt{3}} F_{p,rec} \quad (12)$$

assuming infinite area and same insulation thickness.

In our comparison, we assume a given area and a given packing factor (the ratio between copper area and total area). We compare three different rectangular winding types to a hexagonally packed with the distance between wire centers  $d_0$ : The first one is rectangularly packed with:

$$\begin{aligned} h &= d_0 - d \\ v &= \sqrt{3}d_0/2 - d \end{aligned} \quad (13)$$

The second one is rectangularly packed with:

$$\begin{aligned} v &= d_0 - d \\ h &= \sqrt{3}d_0/2 - d \end{aligned} \quad (14)$$

The third one is a squarely packed winding with:

$$h = v = \sqrt{\sqrt{3}/2} d_0 - d \quad (15)$$

All of the above geometric arrangements result in same packing factor and all have very similar proximity-effect loss factors at low frequencies (for strand diameter less than a skin depth) or at any frequency when the filling factor is low. At high frequencies with high filling factors, FEA results show that, compared to square-packed windings with the same fill factor as setup in (15), hexagonally packed windings have a slightly larger proximity-effect loss factor. However, if the comparison is made with the same spacing between strands, the situation is reversed, and square-packed windings have a slightly higher proximity-effect loss factor than hexagonally packed windings.

Rectangularly packed windings with the same packing factor as the hexagonally packing winding and with unequal vertical and horizontal spacing were also analyzed. Based on previous work [6] we expect lower proximity effect loss factor when the vertical spacing  $v$  (in the direction of the field) is small and when the horizontal spacing  $h$  (perpendicular to the field direction—between layers) is large. As expected, the rectangularly packed winding with large  $h$  and small  $v$  (as in (13)) had low high-frequency proximity effect loss factor, lower than the hexagonally packed winding; and the rectangularly packed winding with large  $h$  and small  $v$  (as in (14)) had high high-frequency proximity effect loss factor, higher than the hexagonally packed winding.

#### IV. COMPLEX PERMEABILITY MODEL FOR LITZ-WIRE BUNDLE

To find the equivalent permeability of a litz-wire winding, we first find the effective permeability of each bundle using the method presented in Section II and Section III. Fig. 8 shows the process of homogenization of litz-wire bundles. In order to find the equivalent permeability of a bundle cell as

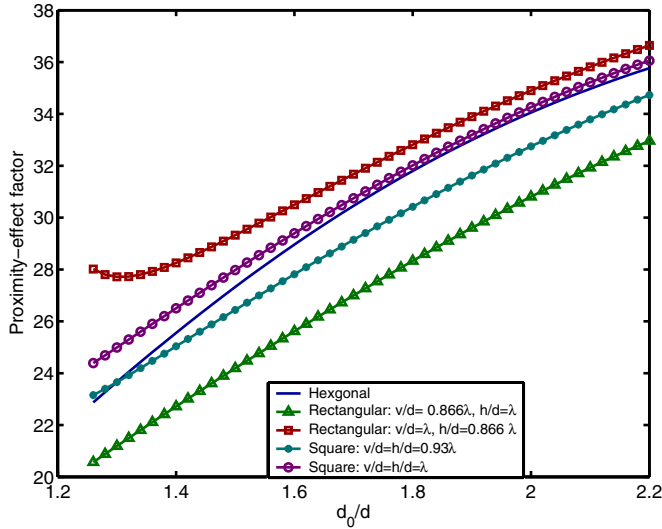


Fig. 7. Comparison of the high-frequency proximity-effect loss factor in a hexagonally packed winding (solid line) with that in different rectangularly packed windings. The line marked with solid circles, below the line for hexagonally packed windings, represents a square-packed winding with the spacing between wires,  $d_0$ , the same as in the hexagonally packed winding. The line marked with open circles, above the line for hexagonally packed windings, represents a square-packed winding with the same packing factor as the hexagonally packed winding, as specified in (15). The top and bottom lines, marked with squares and triangles, represent rectangularly packed configurations that are not square, as specified in (14) and (13), respectively. All curves are for  $d/\delta = 16$ .

defined by (1), we perform FEA simulation on the magnetostatic problem represented by Fig. 8. The equivalent permeability is determined by two variables: the permeability of the litz-wire bundle (circular area)  $\mu_1$  and the area ratio  $r_s$  which is defined as:

$$r_s = \frac{A_{bundle}}{A_{cell}}. \quad (16)$$

in Fig. 8.  $A_{bundle}$  is the area of a circular bundle, and  $A_{cell}$  is the area of the square-shaped bundle cell. FEA results are shown in Fig. 9. The relationships between  $\mu_{avg}$  and these two variables are approximately linear when  $\mu_1$  isn't too small (larger than 0.3) and the area ratio is not too large (smaller than 0.75).

Fig. 10 shows two geometry situations under which average permeability of the setups can be easily determined. The average permeability of a block of material with relative permeability  $\mu_1$  and air can be given as:

$$\mu_{e1} = \mu_1 r_s + 1 - r_s \quad (17)$$

for (a) in Fig. 10, and

$$\mu_{e2} = \frac{\mu_1}{\mu_1(1 - r_s) + r_s} \quad (18)$$

for (b) in Fig. 10, where  $r_s$  is the area ratio of the block with permeability  $\mu_1$ . Calculations in (17) and (18) are based on the assumptions that the field at the boundaries of the two blocks are either parallel to the boundary as in (a) or perpendicular to the boundary as in (b). Neither assumption can be applied to the geometry of a litz-wire bundle in Fig. 8. We compared the

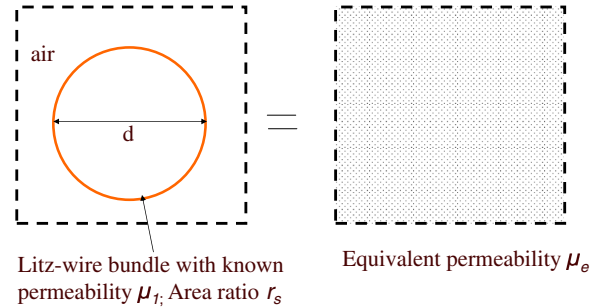


Fig. 8. Homogenization of litz-wire bundles

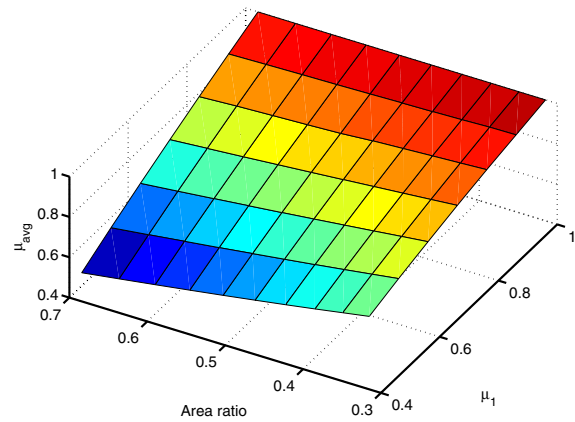


Fig. 9. This figure shows the FEA simulation results of average permeability  $\mu_{avg}$  of a square block consisting a circular region with permeability  $\mu_1$  surrounded by air. The average permeability changes with  $\mu_1$  and the area ratio  $r_s$  of the circular region. From the figure, the relationships between  $\mu_{avg}$  and these two variables are approximately linear when  $\mu_1$  isn't too small (larger than 0.3) and the area ratio is not too large (smaller than 0.75).

average permeabilities given by (17), (18) and the equivalent permeability given by FEA for various sets of  $\mu_1$  and  $r_s$ . The comparison shows that both (17) and (18) are accurate for the geometry in Fig. 8 at extreme case where  $\mu_1 = 1$  or  $r_s = 0$ . However, using (17) overestimates the equivalent permeability and using (18) underestimates the equivalent permeability. The errors of simple area-weighting averaging methods in (17) and (18) can be as large as 20% for large  $r_s$  and small  $\mu_1$ , as shown in Fig. 11 and Fig.12.

A simple combination of the two area-weighting averaging methods can improve the prediction accuracy:

$$\mu_e = w_t \mu_{e1} + (1 - w_t) \mu_{e2} \quad (19)$$

where  $\mu_e$  is the average permeability of a square area containing a circular area with permeability  $\mu_1$  in the center, and  $r_s$  is the area ratio of the round shape. The value of  $w_t$  is varied to achieve best fitting to FEA data and is found to be 0.68 at the smallest total error.

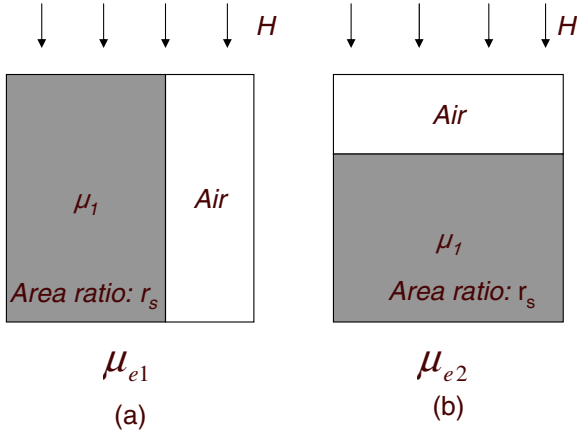


Fig. 10. Two simple geometry situations under which average permeability can be easily found

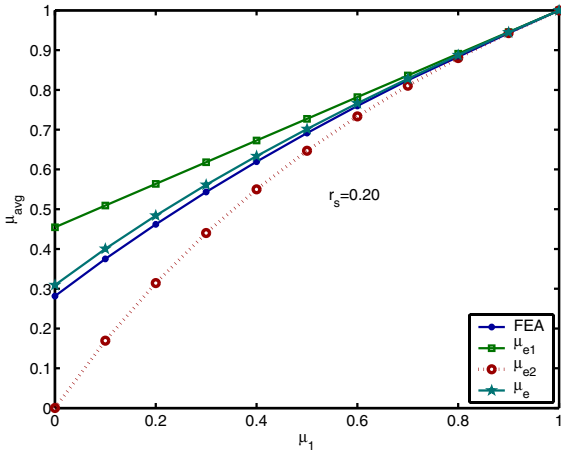


Fig. 11. This figure compares the FEA simulation results of average permeability  $\mu_{avg}$  with the predictions of two area-weighting averaging methods in (17), (18) and the combination of (17) and (18) in (19) for area ratio  $r_s = 0.20$  and various  $\mu_1$ .

Using (19) to predict  $\mu_{avg}$  produces less than 1% error relative to FEA results for  $\mu_1 \geq 0.2$  and  $r_s \leq 0.55$ . For larger area ratio  $r_s$  up to 0.74 (Note the maximum  $r_s$  is  $\pi/4$ ), the error increases slightly but remains within 5%. We checked the possible insulation between strands in litz-wire windings and the corresponding permeabilities based on the simulation results in Section II. The real part of complex permeability is larger than 0.5 for a bundle consisting of single build insulated strands up to the frequency where  $d/\delta$  is 60. The area ratio  $r_s$  is always less than  $\pi/4$  and usually smaller with served litz-wire bundles. Furthermore, in some litz-wire windings thick insulation between layers is used; thus there would be extra spaces between the square bundle cells, which is similar as the setup shown in Fig. 10. Simple averaging as in (17) can be combined with (19) to find the average permeability of these

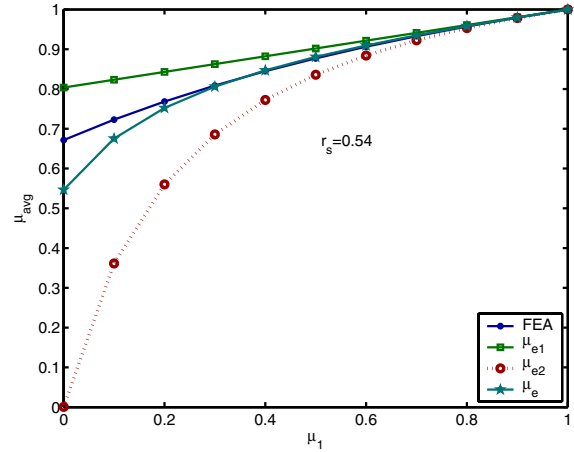


Fig. 12. This figure compares the FEA simulation results of average permeability  $\mu_{avg}$  with the predictions of two area-weighting averaging methods in (17), (18) and the combination of (17) and (18) in (19) for area ratio  $r_s = 0.54$  and various  $\mu_1$ . Averaging method in (17) overestimates the equivalent permeability, while averaging method 2 (18) underestimates the equivalent permeability of the geometry setup in Fig. 8. The combination of them can give a pretty good prediction of equivalent permeability  $\mu_e$ .

windings.

## V. CONCLUSION

In this paper, a complex permeability model for proximity effects in high-frequency litz-wire windings is presented. The model is derived from the proximity-effect loss model based on high-accuracy numerical simulation data. Models for two different strands-packing patterns—rectangularly packing and hexagonally packing—are presented and discussed. Homogenization of litz-wire bundles is also discussed. This permeability model enables high-accuracy proximity-effect loss analysis and field analysis for litz-wire windings at high frequencies and is much more time-efficient than numerical methods.

## APPENDIX

The expressions for  $\hat{G}$ ,  $b$ ,  $k$  and  $w$  are given in [7].

$$\hat{G}(X) = (1 - w) \frac{3\pi}{16} k^{-3} X \frac{\sinh(kX) - \sin(kX)}{\cosh(kX) + \cos(kX)} + w \frac{\pi}{32} \frac{X}{(X^{-3} + b^3)} \quad (20)$$

$$b(v/d, h/d) = f\left(v/d, f(h/d, s_{1b,1}, s_{2b,1}, q_{b,1}), f(h/d, s_{1b,2}, s_{2b,2}, q_{b,2}), f(h/d, s_{1b,3}, s_{2b,3}, q_{b,3})\right) \quad (21)$$

$$k(v/d, h/d) = f\left(h/d, f(v/d, s_{1k,1}, s_{2k,1}, q_{k,1}), f(v/d, s_{1k,2}, s_{2k,2}, q_{k,2}), f(v/d, s_{1k,3}, s_{2k,3}, q_{k,3})\right) \quad (22)$$

$$w(v/d, h/d) = (h/d)w_1(v/d) + w_2(v/d) \\ w_1(v/d) = c_{11} - (u_{11} - u_{01}e^{-\frac{v/d}{\gamma_{01}}})^2 \\ w_2(v/d) = c_{21} + (u_{21} - u_{02}e^{-\frac{v/d}{\gamma_{02}}})^2 \quad (23)$$

where:

$$f(Y, s_1, s_2, q) = \frac{s_1 - s_2}{Y^{-1} + q^{-1}} + s_2 \quad (24)$$

The parameters in (21), (22) and (23) are in Table. I.

TABLE I  
PARAMETERS FOR  $b$ ,  $k$  AND  $w$  TO BE USED IN (21), (22) AND (23)

$b$		$s_{1b,j}$	$s_{2b,j}$	$q_{b,j}$
	$j = 1$	-0.0037	0.0432	-0.0661
	$j = 2$	1.8167	0.0074	0.2195
	$j = 3$	0.7053	0.8378	23.8755
$k$		$s_{1k,j}$	$s_{2k,j}$	$q_{k,j}$
	$j = 1$	1.0261	0.8149	9.3918
	$j = 2$	0.4732	0.8023	1.2225
	$j = 3$	0.0930	0.2588	-0.0334
$w$	$c_{11} = 0.0462$	$u_{11} = 0.1558$	$u_{01} = 0.3477$	$Y_{01} = 1.0673$
	$c_{21} = 0.0018$	$u_{21} = 0.1912$	$u_{02} = 0.2045$	$Y_{02} = 1.3839$

#### REFERENCES

- [1] E. C. Snelling, *Soft Ferrites, Properties and Applications*, Butterworths, second edition, 1988.
- [2] Charles R. Sullivan, "Optimal choice for number of strands in a litz-wire transformer winding", *IEEE Transactions on Power Electronics*, vol. 14, no. 2, pp. 283–291, 1999.
- [3] P. N. Murgatroyd, "Calculation of proximity losses in multistranded conductor bunches", *IEE Proceedings, Part A*, vol. 36, no. 3, pp. 115–120, 1989.
- [4] J.A. Ferreira, "Analytical computation of ac resistance of round and rectangular litz wire windings", Jan 1992.
- [5] N.; Reatti A.; Kazimierczuk M.K. Bartoli, M.; Noferi, "Modeling litz-wire winding losses in high-frequency power inductors".
- [6] Xi Nan and Charles R. Sullivan, "An improved calculation of proximity-effect loss in high frequency windings of round conductors", in *34th Annual IEEE Power Electronics Specialists Conference*, 2003, vol. 2, pp. 853–860.
- [7] Xi Nan and Charles R. Sullivan, "Simplified high-accuracy calculation of eddy-current loss in round-wire windings", in *35th Annual IEEE Power Electronics Specialists Conference*, 2004, vol. 2, pp. 873 – 879.
- [8] Richard L. Stoll, *The analysis of eddy currents*, Clarendon Press. Oxford, 1974.
- [9] O. Moreau, L. Popiel, and J.L. Pages, "Proximity losses computation with a 2d complex permeability modelling", *IEEE Transactions on Magnetics*, vol. 34, pp. 3616–3619, 1998.
- [10] Xi Nan and Charles R. Sullivan, "A two-dimensional equivalent complex permeability model for round-wire windings", 2005.